

Nontrivial Haldane phase of an atomic two-component Fermi gas trapped in a 1d optical lattice

Keita Kobayashi,^{1,2} Masahiko Okumura,^{1,2,3,4} Yukihiro Ota,⁵ Susumu Yamada,^{1,2,4} and Masahiko Machida^{1,2,4}

¹CCSE, Japan Atomic Energy Agency, 5-1-5 Kashiwanoha, Kashiwa, Chiba 277-8587, Japan

²CREST(JST), 4-1-8 Honcho, Kawaguchi, Saitama 332-0012, Japan

³Computational Condensed Matter Physics Laboratory, RIKEN, Wako, Saitama 351-0198, Japan

⁴Computational Materials Science Research Team, RIKEN AICS, Kobe, Hyogo 650-0047, Japan

⁵Advanced Research Institute, RIKEN 2-1 Hirosawa, Wako-shi, Saitama 351-0198, JAPAN

(Dated: September 26, 2018)

We propose how to create a non-trivial Haldane phase in atomic two-component Fermi-gas loaded on one-dimensional (1-D) optical lattice with trap potential. The Haldane phase is naturally formed on p -band Mott core in a wide range of the strong on-site repulsive interaction. The present proposal is composed of two steps, one of which is theoretical derivation of an effective 1-D $S = 1$ interacting-chain model from the original tight-binding Hamiltonian handling the two p -orbitals, and the other of which is numerical demonstration employing the density-matrix renormalization-group for the formation of the Haldane phase on p -band Mott core and its associated features in the original tight-binding model with the harmonic trap potential.

PACS numbers: 67.85.Lm, 03.75.Ss, 71.10.Fd, 75.40.Mg

Ultra-cold Fermi gas loaded on optical lattice (FGOL) is one of the most fascinating systems in modern physics [1]. Its controllability is far beyond our past image and experience in condensed matters. For instance, the two-body interaction between Fermi atoms is widely variable from strongly attractive to repulsive. Moreover, filling and population imbalance are freely tunable, and lattice geometry is highly flexible. Thus, FGOL is regarded as an outstanding simulator for strongly-correlated electronic materials, in which a great number of controversial issues like high-temperature superconducting mechanism in cuprate superconductors still remain unsolved.

Very recently, there have been intense theoretical and experimental interests in extending the energy band produced by the optical lattice (OL) potential from the ground single one to higher multiple-ones by utilizing multi-degenerate higher orbitals [2, 3]. Such multiple orbital degeneracy allows us to study orbital degrees of freedom in addition to charge and spin ones. Then, FGOL becomes a more realistic and rich simulator, in which orbital ordering and high-spin correlation are accessible subjects like real solid-state matters including transition metals and other heavy elements [4, 5]. In this paper, we study one of the most fundamental issues associated with the multiple band degeneracy. The present target is formation of a gapped quantum phase using double p -orbital degeneracy under a one-dimensional(1-D) system, as shown in Fig.1. We show that an effective low-energy Hamiltonian is given by the $S = 1$ Heisenberg model and the gapped Haldane phase [6] is widely sustained by the harmonic trap potential to confine Fermi atoms. The fertility of the Haldane phase, i.e., gapful spin-excitation, nonlocal string order, and spin-1/2 edge magnetization induction [7–10] can be systematically explored because of the wide controllability in FGOL's.

Feasibility studies to create the Haldane phases in atomic gas OL's have been made on spin 1 bosonic gases

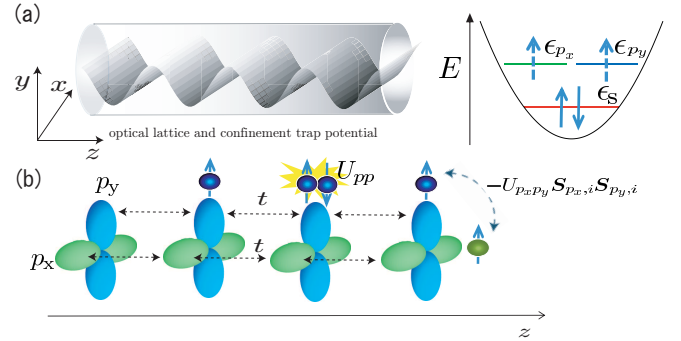


FIG. 1: (Color Online) Schematic figures for a 1-D Fermi gas. (a) An optical lattice (OL) potential along z -direction and a cylindrically-symmetric vertical trap-potential inside xy -plane. The latter causes to form discrete levels as depicted at the right panel, in which the lowest level is s -orbital while higher two degenerate ones are $p_{x,y}$ -orbitals. The Haldane phase is formed under fully-filled s - and partially-filled p -orbitals (see text). (b) $p_{x,y}$ -orbitals formed inside the vertical trap and their p -bands created by the OL. When p -bands are active, this system is described by a multi-band Hubbard chain with the on-site intra-orbital interaction (U_{pp}) and inter-orbital one ($U_{p_x p_y}$) (see Eq.(2) and text).

loaded on 1-D OL with one atom per site [11], two-component 1-D FGOL utilizing 1st and 2nd Bloch-bands with Feshbach resonance [12], and ultra-cold fermionic ^{171}Yb in 1-D OL [13]. The Haldane insulator, in which a charge gap opens according to Haldane's conjecture [6], was also predicted for bosonic gases with dipole interaction [14–16] and multi-component 1-D FGOL [17]. In this paper, through the derivation of an effective $S = 1$ interacting-chain model and the numerical simulations of a multi-band Hubbard model, we show that the Haldane phase is naturally formed in a two-component 1-D FGOL

with the emergence of p -band Mott core. We also reveal features of the Haldane phase in trapped systems.

We start with the following Hamiltonian describing a 1-D elongated FGOL schematically depicted in Fig.1,

$$H = \sum_{\sigma=\uparrow,\downarrow} \int d\mathbf{x} \left[\psi_{\sigma}^{\dagger} h_0 \psi_{\sigma} + \frac{g}{2} \psi_{\sigma}^{\dagger} \psi_{\bar{\sigma}}^{\dagger} \psi_{\bar{\sigma}} \psi_{\sigma} \right], \quad (1)$$

with $h_0 = (-\hbar^2/2m)\nabla^2 + V_{\text{ver}} + V_{\text{opt}}$ and the coupling constant of the two-body interaction g . The cylindrically-symmetric vertical trap (on xy -plane) and the OL potential (along z -axis) are, respectively, V_{ver} and V_{opt} .

A multi-band Hubbard-type model is derived from Eq.(1) using the expansion $\psi_{\sigma} = \sum_{\alpha,\beta} \sum_i c_{\alpha,\beta,\sigma,i} u_{\alpha} w_{\beta,i}$, where u_{α} and $w_{\beta,i}$ are a wavefunction associated with the eigensystem of $[(-\hbar^2/2m)\nabla_{\perp}^2 + V_{\text{ver}}] u_{\alpha} = \epsilon_{\alpha} u_{\alpha}$ and a Wannier function formed by the OL potential. The indices α and β represent discrete levels caused by the trap potential V_{ver} and Bloch-band by the OL potential, respectively. Here, V_{ver} is not so tight that the 2nd p -orbital energy-level does not exceed over that of 2nd Bloch-band and the 2nd level is partially filled, as shown in Fig.1(b). Hereafter, ignoring the contribution from higher Bloch-bands, we drop the index β . Then, including the 2nd level corresponding to $p_{x(y)}$ -orbital and taking the tight-binding approximation, we obtain a multi-band 1-D Hubbard Hamiltonian [18]

$$\begin{aligned} H = & - \sum_{\alpha,\sigma} \sum_{\langle i,j \rangle} t c_{\alpha,\sigma,i}^{\dagger} c_{\alpha,\sigma,j} + \sum_{\alpha,\sigma,i} \epsilon_{\alpha} n_{\alpha,\sigma,i} \\ & + \sum_i \left[\sum_{\alpha} U_{\alpha\alpha} n_{\alpha,\uparrow,i} n_{\alpha,\downarrow,i} - \sum_{\alpha \neq \alpha'} U_{\alpha\alpha'} \left\{ \mathbf{S}_{\alpha,i} \cdot \mathbf{S}_{\alpha',i} \right. \right. \\ & \left. \left. - c_{\alpha,\uparrow,i}^{\dagger} c_{\alpha,\downarrow,i}^{\dagger} c_{\alpha',\downarrow,i} c_{\alpha',\uparrow,i} - \sum_{\sigma,\sigma'} \frac{1}{4} n_{\alpha,\sigma,i} n_{\alpha'\sigma',i} \right\} \right], \quad (2) \end{aligned}$$

where $n_{\alpha,\sigma,i} (\equiv c_{\alpha,\sigma,i}^{\dagger} c_{\alpha,\sigma,i})$ is the on-site number-density operator of α -orbital with pseudo-spin σ and $\mathbf{S}_{\alpha,i} = \frac{1}{2} \sum_{\sigma,\sigma'} c_{\alpha,i,\sigma}^{\dagger} \boldsymbol{\tau}_{\sigma,\sigma'} c_{\alpha,i,\sigma'}$ with Pauli matrices $\boldsymbol{\tau}$ is the local spin-1/2 operator. The summation of α is taken from the ground s -orbital to the 2nd degenerate p -orbitals (p_x and p_y) as shown in Fig.1(c). t and $U_{\alpha\alpha'}$ are the hopping and on-site interaction energy integrals defined as $t = - \int dz w_{i+1} \left(\frac{-\hbar^2}{2m} \frac{\partial^2}{\partial z^2} + V_{\text{opt}} \right) w_i$ and $U_{\alpha\alpha'} = g \int d\mathbf{x} w_i^{\dagger} u_{\alpha}^2 u_{\alpha'}^2$, respectively. The in-plane cylindrical symmetry of $u_{\alpha}(\mathbf{x}_{\perp})$ gives the relations $U_{sp_x} = U_{sp_y} (\equiv U_{sp})$ and $U_{p_x p_x} = U_{p_y p_y} (\equiv U_{pp})$. A significant feature in Eq.(2) is the existence of Hund's like terms $-U_{\alpha\alpha'} \mathbf{S}_{\alpha,i} \cdot \mathbf{S}_{\alpha',i}$, which captures the so-called orbital physics. Similar Hamiltonian to Eq.(2) may also appear in ultra-cold fermionic ^{171}Yb with 1S_0 - and 3P_0 -states [13, 19].

Now, we derive a $S = 1$ Heisenberg chain from Eq.(2) in the strong coupling limit ($U_{\alpha\alpha'} \gg t$). We consider a case when the 1st orbital is fully occupied and 2nd ones are half-filled. Now, this system seem to be

similar to two Heisenberg chains coupled by ferromagnetic exchange interaction, which can produce the Haldane phase [20]. In fact, the second order perturbation scheme [21] leads to $H_J = J_{\text{ex}} \sum_{\langle i,j \rangle} \mathbf{S}_i \cdot \mathbf{S}_j$, where $J_{\text{ex}} = 2t^2/(U_{pp} + U_{p_x p_y})$ and the local spin-1 operator $\mathbf{S}_i = \frac{1}{2} \sum_{\alpha=p_x, p_y} \sum_{\sigma,\sigma'} c_{\alpha,\sigma',i}^{\dagger} \boldsymbol{\tau}_{\sigma'\sigma} c_{\alpha,\sigma,i}$ [18]. Hence, a gapped Haldane phase can emerge for large U_{pp} if the 2nd p -levels are half-filled. In FGOL experiments, this requirement is achievable in a central Mott core formed by interplay between a trap potential and large U_{pp} .

Next, let us turn to the numerical demonstration of the Haldane phase by the density-matrix renormalization-group (DMRG) method [22, 23]. Typical atomic-gas experiments employ harmonic trap potential in all directions to prevent escape of atoms. We add the harmonic trap along z -axis, $V_{\text{ho}}(i) = V[2/(L-1)]^2 [i - (L+1)/2]^2$ to our system, as well as the aforementioned vertical trap V_{ver} . Here L means the total number of sites. The total Hamiltonian is $H + \sum_{\alpha,\sigma,i} V_{\text{ho}}(i) n_{\alpha,\sigma,i}$. Again, we drop off the terms in the Hamiltonian relevant with the 1st orbital [18]. We simulate the model handling only 2nd p -orbitals [24]. In the 2-band Hubbard model, the on-site intra-orbital interaction U_{pp} and inter-orbital interaction $U_{p_x p_y}$ are mutually connected via $U_{p_x p_y} = \frac{4}{9} U_{pp}$. We note that $U_{\alpha\alpha'} = g \int d\mathbf{x} w_i^{\dagger} u_{\alpha}^2 u_{\alpha'}^2$, [25].

Now, we present numerical results. We obtain a particle-density distribution $n(i) = \sum_{\alpha=p_x, p_y, \sigma} n_{\alpha,\sigma,i}$ and a spin-density distribution $m(i) = \sum_{\alpha=p_x, p_y} (n_{\alpha,\uparrow,i} - n_{\alpha,\downarrow,i})$ using DMRG simulations. Figure 2(a) shows $n(i)$ for $U_{pp}/t = 15$ and $V/t = 10$. Owing to $V_{\text{ho}}(i)$, p -band Mott plateau is formed in the trap center and surrounded by regions with trap-gradient-dependent filling (below half). Varying an input imbalance ratio $p \equiv \sum_i m_i/n_i$, which is initially set in experiments, we measure the normalized polarization on the Mott core [26], $M = \sum_{i \in \text{Mott}} m_i/n_i$, as seen in Fig.2(b). For comparison, we also show in the inset the result for $U_{p_x p_y} = 0$, which corresponds to two identical 1-D Hubbard chains without coupling. A plateau-like behavior occurs on the Mott-core polarization up to a critical imbalance ratio $p_c (\simeq 0.17)$ as expected in the presence of the gap, while for $U_{p_x p_y} = 0$ the Mott-core is smoothly magnetized. A gapful phase for the spin flip excitation is found in the p -band Mott-core region. Thus, one of the key features of the Haldane phase is shown.

Let us more carefully examine the trap center and the outer regions for a balanced case $p = 0$ ($S_{\text{tot}}^{(z)} (\equiv \sum_i S_i^{(z)}) = 0$) and a slightly-polarized case $p = 0.0125$ ($S_{\text{tot}}^{(z)} = 1$). First, we focus on the spin-density distribution profiles on the p -band Mott core. Figure 3 shows that staggered magnetization structures emerge at the edges of the p -band Mott core and exponentially decay toward the trap center. This structure is the same as the typical one observed at open boundary edges in $S = 1$ Heisenberg chains [9, 10] and is known to be induced by $S = 1/2$ fraction left at open bound-

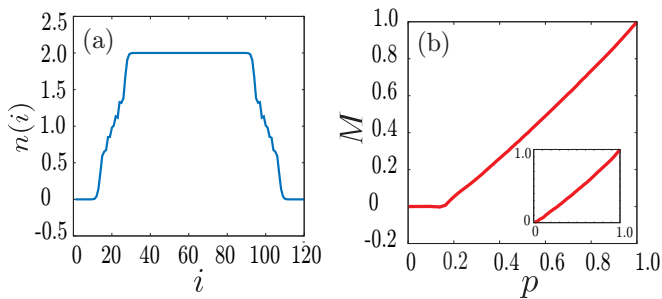


FIG. 2: (Color Online) (a) A typical spatial distribution profile of the particle density $n(i) = \sum_{\alpha=p_x, p_y} \sum_{\sigma} n_{\alpha, \sigma, i}$ for balanced 160 fermions (80 \uparrow , 80 \downarrow) with the interaction constants $U_{pp}/t = 15$, $U_{p_x p_y} = \frac{4}{9}U_{pp}$, and the trap potential strength $V/t = 10$. (b) The Mott-core polarization M vs. the population imbalance ratio p . The employed parameters are the same parameter as in (a) except for p . For comparison, the inset is the case of $U_{pp}/t = 15$ and $U_{p_x p_y}/t = 0$, which is equivalent with two independent $S = 1/2$ interacting chains.

ary edges. In the present case, the p -band Mott core is not sharply terminated by the open boundary condition. The edge magnetization amplitude in the induced staggered structures is sizeably reduced, compared to the results of $S = 1$ Heisenberg chain in the open boundary case [9]. This difference comes from coupling between $S = 1/2$ fraction left at the edges of the p -band Mott core and a ferromagnetic metallic phase in the outer regions. The ferromagnetic property in the outer regions is confirmed by calculating spin-gap energy $\Delta E_p = E_p - E_{p=0}$, polarization on outer regions, and the Mott-core polarization [18]. Here, E_p is the ground-state energy for the population imbalance ratio p . This ferromagnetism is also consistent with theoretical prediction for a uniform hole-doped two-degenerate-band system with strong Hund's coupling [27]. Next, let us examine the outer regions to understand coupling between the ferromagnetic metal and the $S = 1/2$ fraction at the edge of the Mott core. As for $S_{\text{tot}}^{(z)} = 0$, as shown in Fig. 3(a), the spin-density profile is anti-centrosymmetric. We calculate the integral of $m(i)$ over the left (right) outer region, $m_{L(R)} \equiv \sum_{i \in \text{left(right)}} m(i)$. Then, we find that the left and right regions, respectively, are polarized as one up-spin ($m_L \simeq 1$) and one down-spin ($m_R \simeq -1$). For $S_{\text{tot}}^{(z)} = 1$, as shown in Fig. 3(b), both regions are polarized as one up-spin ($m_L = m_R \simeq 1$). We always find similar features for various p . The polarization difference becomes either $|m_L - m_R| \simeq 0$ or $|m_L - m_R| \simeq 2$ as shown in Fig. 3(c). These results mean that $S = 1/2$ fractions left at the edges of the p -band Mott core may spread over the outer regions. We further characterize the ferromagnetic metal on the outer regions. We compare the spin-gap energy with Mott-core polarization. The ground-state degeneracy (i.e., $\Delta E_p = 0$) exists up to $p \simeq 0.11$, as seen in Fig. 3(d), while plateau-like behavior in Fig. 2(b) still continues up to $p \simeq 0.17$. This result implies that all

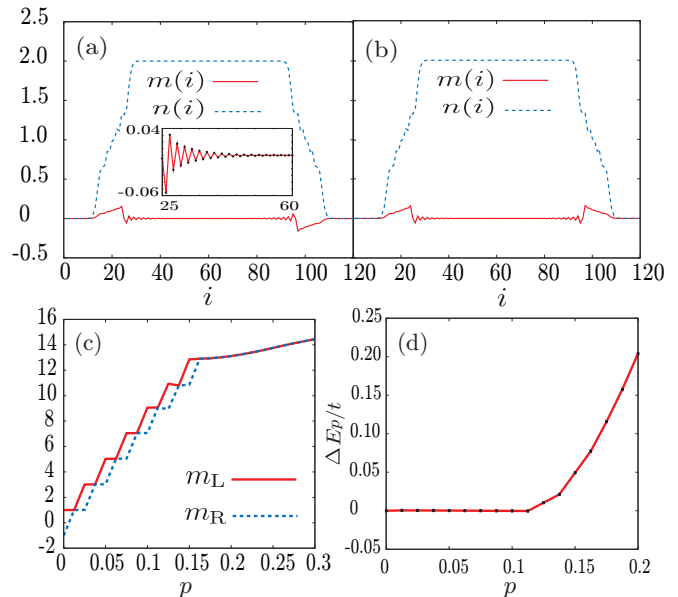


FIG. 3: (Color Online) Distribution profiles of particle density (dashed blue line) $n(i)$ and spin density (solid red line) $m(i) = \sum_{\alpha=p_x, p_y} (n_{\alpha, \uparrow, i} - n_{\alpha, \downarrow, i})$ for spin imbalance (a) $p = 0$, ($S_{\text{tot}}^{(z)} = 0$) and (b) $p = 0.0125$, ($S_{\text{tot}}^{(z)} = 1$). The inset of (a) is a focus on the spin density around the edge of the left Mott core. (c) The polarization in the left (right) surrounding phase $m_{L(R)} \equiv \sum_{i \in \text{left(right)}} m(i)$ versus the population imbalance ratio p . (d) The spin gap $\Delta E_p \equiv E_p - E_{p=0}$ versus the population imbalance ratio p . All other physical parameters are the same as in Fig. 2(a).

spin degrees of freedom in the system accumulate on the ferromagnetic metal before $p \simeq 0.11$. Therefore, the ferromagnetic metal on the outer regions corresponds to an edge state in uniform $S = 1$ Heisenberg model.

Here, we mention the case of small U_{pp}/t . The Haldane phase may survive in small U region as discussed in the case of multi-component 1-D FGOL [17]. We emphasize that, for a wide-range of the interaction strength and the trap potential strength V/t , the gapped Mott core more or less appears and the Haldane phase is realized in the central core region [18].

We further increase the population imbalance ratio to examine the spin-density distribution profiles before and after p_c . As for $p = 0.1625$ ($N_{\uparrow} - N_{\downarrow} = 26$), as seen in Fig. 4(a), the central Mott core is not magnetized, and all the polarization concentrates on the ferromagnetic metallic phases, while the magnetization amplitude is considerably enhanced compared to Fig. 3. A coupling with the Haldane phase and polarized ferromagnetic metal brings about the enhancement of the edge magnetization. On the other hand, when $p = 0.475 (> p_c)$, the staggered structure disappears, and even the p -band Mott core is uniformly magnetized, as shown in Fig. 4(b). As for an extremely population imbalance ratio $p = 0.9375$, a periodical oscillation appears inside the p -band Mott core

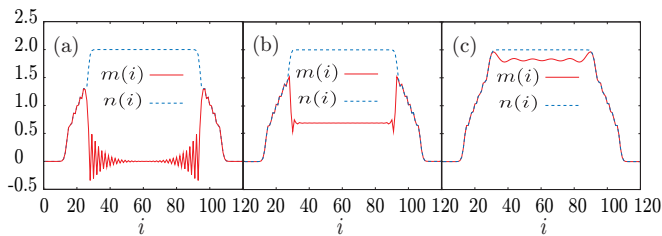


FIG. 4: (Color Online) Particle density (dashed blue line) and spin density (solid red line) distribution profiles for population imbalance ratios (a) $p = 0.1625$ (93 \uparrow , 67 \downarrow), (b) $p = 0.475$ (118 \uparrow , 42 \downarrow), and (c) $p = 0.9375$ (155 \uparrow , 5 \downarrow). All other parameters are the same as in Fig.2 (a).

as shown in Fig.4(c). This oscillation can be explained as follows. A low-energy excitation of the spin- S Heisenberg model under strong magnetic field is described by the Luttinger liquid irrespective of the spin length S [28]. Then, this theoretical picture predicts that the periodicity of a spin-density wave (SDW) is characterized by $2k_F$, where k_F is the Fermi wave vector in the equivalent spinless fermion system. In the present trapped systems, the oscillation periodicity is given by the relation $2k_F = (2\pi/L_{\text{Mott}})N_{\text{Mott},\downarrow}$ [28, 29], where L_{Mott} is the size of the Mott core, and $N_{\text{Mott},\downarrow}$ is the total number of spin-down component inside the Mott-core. Indeed, the magnetization profile shows an expected oscillation.

In Fig.4(c), the number of the minimum peaks of the SDW is 5. This number should be almost equal to $N_{\text{Mott},\downarrow}$. In fact, we can directly evaluate $N_{\text{Mott},\downarrow}$ and find $N_{\text{Mott},\downarrow} \simeq 5$. A more systematic analysis on p -dependence in such a SDW-like oscillation is shown in Ref. [18].

In conclusion, we confirmed that the Haldane phase emerges as a leading phase when utilizing 2nd degenerate p -orbitals in 1-D FGOL. At the half-filling condition for p -orbitals in the large U limit, the multi-band Hubbard Hamiltonian was reduced to the $S = 1$ Heisenberg chain model. Then, the emergence of the Haldane phase and its associated physics were demonstrated by DMRG studies on the original model together with the harmonic trap potential. The polarization on the outer regions is easily observed in experiment [30, 31] and spin-selective single-site addressing [32] can be used to detect the staggered magnetization on Mott core. The formation of the Haldane phase in 1-D FGOL allows us to not only investigate its features but also open a new avenue towards topologically-protected quantum state engineering [33].

We wish to thank T. Morimae, H. Onishi and R. Igarashi for their useful discussions. This work was partially supported by the Strategic Programs for Innovative Research, MEXT, and the Computational Materials Science Initiative, Japan. The numerical work was partially performed on Fujitsu BX900 in JAEA. We acknowledge their supports from CCSE staff.

-
- [1] See for reviews, e.g., I. Bloch, J. Dalibard, and W. Zwerger, *Rev. Mod. Phys.* **80**, 885 (2008); M. Lewenstein, A. Sanpera, B. Damski, A. Sen(De), and U. sen, *Adv. Phys.* **56**, 243 (2007), and references therein.
- [2] Torben Müller, Simon Fölling, Artur Widera, and Immanuel Bloch, *Phys. Rev. Lett.* **99**, 200405 (2007).
- [3] Georg Wirth, Matthias Ölschläger, and Andreas Hemmerich, *Nature. Physcis.* **7**, 147, (2011).
- [4] Kai Wu and Hui Zhai, *Phys. Rev. B* **77**, 174431 (2008).
- [5] Congjun Wu, *Phys. Rev. Lett.* **100**, 200406 (2008).
- [6] F. D. M. Haldane, *Phys. Lett. A* **93**, 464 (1983); *Phys. Rev. Lett* **50**, 1153 (1983).
- [7] H. Tasaki *Phys. Rev. Lett.* **66**, 798 (1991); T. Kennedy and H. Tasaki, *Phys. Rev. B* **45**, 304 (1992); *Commun. Math. Phys.* **147**, 431 (1992).
- [8] I. Affleck, T. Kennedy, E. H. Lieb, and H. Tasaki, *Phys. Rev. Lett.* **59**, 799 (1987); *Commun. Math. Phys.* **115**, 477 (1988).
- [9] S. Miyashita and S. Yamamoto, *Phys. Rev. B* **48**, 913, (1993).
- [10] F. Tedoldi, R. Santachiara, and M. Horvatic, *Phys. Rev. Lett.* **83**, 412 (1999).
- [11] J. J. Garcia-Ripoll, M. A. Martin-Delgado, and J. I. Cirac, *Phys. Rev. Lett.* **93**, 250405 (2004).
- [12] A. F. Ho, *Phys. Rev. A* **73**, 061601(R) (2006).
- [13] H. Nonne, E. Boulat, S. Capponi, P. Lecheminant, *Phys. Rev. B.* **82**, 155134 (2010).
- [14] Emanuele G. Dalla Torre, Erez Berg, and Ehud Altman, *Phys. Rev. Lett.* **97**, 260401 (2006); Erez Berg, Emanuele G. Dalla Torre, Thierry Giamarchi, and Ehud Altman, *Phys. Rev. B* **77**, 245119 (2008).
- [15] L. Amico *et al.*, *New J. Phys.* **12**, 013002 (2010).
- [16] Yu-Wen Lee *Phys. Rev. B* **77**, 064514 (2008).
- [17] H. Nonne, P. Lecheminant, S. Capponi, G. Roux, and E. Boulat, *Phys. Rev. B.* **81**, 020408(R) (2010); *Phys. Rev. B.* **84**, 125123 (2011).
- [18] See supplementary material at [URL will be inserted by publisher].
- [19] A. V. Gorshkov, M. Hermele, V. Gurarie, C. Xu, P. S. Julienne, J. Ye, P. Zoller, E. Demler, M. D. Lukin, and A. M. Rey, *Nat. Phys.* **6**, 289 (2010).
- [20] T. Barnes and J. Riera, *Phys. Rev. B.* **50**, 6817 (1994); A. K. Kolezhuk and H.-J. Mikeska, *Phys. Rev. B* **53**, R8848 (1996); Eugene H. Kim, G. Fath, J. Solyom and D. J. Scalapino, *Phys. Rev. B* **62**, 14965 (2000).
- [21] I. Hubač and S. Wilson, *Brillouin-Wigner Methods for Many-Body Systems* (Springer, Heidelberg, 2009).
- [22] S. R. White, *Phys. Rev. Lett.* **69**, 2863 (1992); *Phys. Rev. B.* **48**, 10345 (1993).
- [23] For recent reviews, see, e.g., K. A. Hallberg, *Adv. Phys.* **55**, 477 (2006), Ulrich Schollwöck, *Ann. Phys.* **326**, 96 (2011), and references therein.
- [24] We take the number of states kept $m_s = 400$ in all DMRG calculations on the model. The maximum truncation error is order of 10^{-7} and m_s -dependence of ground-state energy $E(m_s)$ is $[E(400) - E(350)]/Lt \simeq 10^{-7}$.

- [25] We assume that confinement potential in xy -direction is harmonic trap potential $V_{\text{ver}} = (m\omega_{\text{ver}}/2)(x^2 + y^2)$ and evaluate the relation U_{pp} and $U_{p_x p_y}$ analytically.
- [26] M. Okumura, S. Yamada, M. Machida, and T. Sakai, Phys. Rev. A **79**, 061602(R), (2009).
- [27] K. Kubo, J. Phys. Soc. Jpn. **51**, 782 (1982); K. Kusakabe and H. Aoki, Physica B **194**, 217 (1994).
- [28] Gabor Fath, Phys. Rev. B **68**, 134445, (2003).
- [29] M. Machida, M. Okumura, S. Yamada, T. Deguchi, Y. Ohashi, and H. Matsumoto, Phys. Rev. B **78**, 235117, (2008).
- [30] Guthrie B. Partridge, Wenhui Li, Ramsey I. Kamar, Yean-an Liao and Randall G. Hulet, Science **311**, 503 (2006).
- [31] Yean-an Liao, Ann Sophie C. Rittner, Tobias Paprottam Wenhui Li, Guthrie B. Partridge, Randall G. Hulet, Stefan K. Baur and Erich J. Mueller, Nature (London) **467**, 567 (2010).
- [32] C. Weitenberg, M. Endres, J. F. Sherson, M. Cheneau, P. Schaus, T. Fukuhara, I. Bloch, and S. Kuhr, Nature (London) **471**, 319 (2011); C. Weitenberg, P. Schaus, T. Fukuhara, M. Cheneau, M. Endres, I. Bloch, and S. Kuhr, Phys. Rev. Lett. **106**, 215301 (2011).
- [33] Gavin K. Brennen and Akimasa Miyake, Phys. Rev. Lett. **101**, 010502 (2008); Akimasa Miyake, Phys. Rev. Lett. **105**, 040501 (2010).